RECEIVED
DEC 0 8 2003
TC 1700

PATENT

IN THE UNITED STATES PATENT AND TRADEMARK OFFICE

Application of

Application No.	:	09/975,974
Docket No.	:	461987-007
Applicant	:	E. Jennings Taylor
Filed	:	October 15, 2001
Title	:	ELECTRODEPOSITION OF METALS IN HIGH-ASPECT RATIO CAVITIES USING MODULATED REVERSE ELECTRIC FIELDS
Art Unit	:	1753
Examiner	:	Brian L. Mutschler

COMMISSIONER FOR PATENTS
P.O. BOX 1450
ALEXANDRIA VA 22313-1450

Post-it® Fax Note 7671	Date 11/21/2003	# of pages ▶ 14
To Mark Levy	From E.J. Taylor	
Co./Dept. Thompson Hine LLP	Co. Faraday	
Phone # 937-443-6949	Phone # 937-836-7749	
Fax # 937-443-6635	Fax # 937-836-9498	

Sir:

DECLARATION UNDER 37 C.F.R. 1.132 by E. Jennings Taylor

I E. Jennings Taylor declare and state that I am the inventor of the above-identified application. I am also a registered patent agent, Registration No.53,676.

I have a Ph.D. in Materials Science from the University of Virginia (1981) and my dissertation studies focused on electrochemical processes, within which electro-deposition/electro-plating/plating reside.

I have specifically been working in the electro-plating industry since the mid 1980s. I incorporated Faraday Technology Inc. in 1992. Faraday is a R&D firm engaged in inventing and developing electro-chemical processes, more specifically processes for the electronics industry including plating of printed wiring boards and semiconductor devices.

I have reviewed the Official Action dated August 21, 2003 and the rejections under 35 U.S.C. §103(a) over Martin et al., U.S. Patent 6,071,398. In my previous response, as noted at paragraph 12 at page 15 of the Official Action, I pointed out that Martin at column 5, line 24 describes his plating bath as a "standard copper plating solution." Based upon my experience, as well as literature documents,[1] "standard" plating solutions routinely contain a source of the metal, e.g. copper sulfate, a supporting electrolyte, e.g. sulfuric acid, and a system of additives.

These additives generally include, a carrier (sometimes referred to as a suppressor), e.g. polyethylene glycol, a halide, e.g. chloride and at least one of a leveler or a brightener.

> *"Brighteners are responsible for the formation of small-grained, bright deposits. They function by preventing the deposition of copper at preferred locations by enhancing the formation of new deposit nuclei as opposed to the build-up of existing nuclei."*[2]

> *"[Levelers] act through selective adsorption on readily accessible surfaces (i.e., flat field areas and protruding high points."*[3]

Regarding the need for these additive constituents,

"Used alone, these additives have a minimal effect on the leveling of the deposit; however, formulated together they impart a synergistic effect that maximizes leveling effects."[4]

The solutions described in the examples in the Martin patent all contain copper sulfate, sulfuric acid, chloride, "PPR carrier" and an additive identified as "PPR additive." Based upon my experience as one of ordinary skill in the art, the "PPR additive" is either a leveler or brightener.

As I indicated, I am also a registered patent agent. At paragraph 13 of the Office Action, the Office contends that claim 4 in the Martin patent teaches electroplating baths that do not require levelers or brighteners. However, based upon my experience in the electroplating field and as a patent agent, a person skilled in the art would not interpret claim 4 as teaching plating solutions that do not contain a leveler or brightener but rather merely interpret claim 4 as a broad characterization of electroplating solutions and not as indicating that solutions without levelers or brighteners are useful. In this regard, claim 4 in the Martin patent is inconsistent and is not supported by the solutions that are used in the examples and which contain both a PPR carrier and a PPR additive in addition to the claimed sulfuric acid, copper sulfate, and chloride ions.

For the reasons indicated herein, a person skilled in the art can not read Martin as teaching the use of plating solutions that do not contain brighteners or levelers.

The method of the present invention is unique because the plating bath is devoid of levelers and brighteners. Based upon my experience in the electroplating field, levelers and

brighteners are associated with several drawbacks. One is their cost but, more importantly, because levelers and brighteners break down during the plating operation, their presence in the plating bath must be carefully monitored. As these additives breakdown, plating conditions change and plating quality diminishes. Consequently, it is essential to schedule maintenance and to periodically replace the plating baths when brighteners and levelers are used. Furthermore, the properties of the electro-deposit may be adversely affected by these additives,

> *"...there is a need to reduce the use of organic additives in printed circuits and in the damascene metallization ... because the material incorporated in the solid phase could damage the electronic properties of the deposit film such as conductivity, ductility, and adhesion."*[5]

The present invention provides a method for plating features in circuit boards having high aspect ratios without using levelers or brighteners through the use of pulsed electric current. The art does not teach or suggest that pulsed current systems can be used effectively to plate high aspect ratio features without brighteners or levelers. This is highly advantageous because it reduces cost and it removes a source of substantial variability in the plating process.

I declare that all statements made herein are true and all statements made herein on information and belief are believed to be true and I understand that willful false statements could render any patent that issues on this application invalid or unenforceable.

Respectfully submitted,

E. Jennings Taylor

Date: August 5, 2003

E. JENNINGS TAYLOR

THOMPSON HINE LLP
2000 Courthouse Plaza NE
10 West Second Street
Dayton, Ohio 45402-1758
PH (937) 443-6949
FX (937) 443-6635

318497

[1] R.D. Mikkola, Q.-T. Jiang & B. Carpender, "Copper Electroplating for Advanced Interconnect Technology" *Plating & Surface Finishing*, **87**(3) 81 March 2000.
[2] Ibid. page 84.
[3] Ibid. page 84.
[4] Ibid. page 84.
[5] K.-M. Yin, "Mathematical Model of Galvanostatic Pulse with Reverse Plating in the Presence of a Surface Blocking Agent" *J. Electrochem. Soc.*, ***150*** *(6) C435-9 (2003).*

Copper Electroplating For Advanced Interconnect Technology

By R.D. Mikkola, Q.-T. Jiang & B. Carpenter

Copper electroplating for gap fill of damascene structures on advanced interconnects has been demonstrated to be a viable technology. Development and optimization of robust electroplating processes for void-free fill requires full understanding of the role of the plating solution components (brighteners, levelers, and suppressing agents) and their behavior as a function of plating amperage, waveform and bath temperature. Methodology for void-free fill of damascene structures will be presented, as well as an interpretation of grain growth transformations and morphological changes for the thin copper films.

The semiconductor industry is moving toward implementation of electroplated copper for metallization of advanced interconnects. Motorola and IBM will have had commercial products utilizing this metallization scheme for sale in 1999. Full integration of electroplated copper into the chip manufacturing process will require optimization and control of a number of key issues (*i.e.*, plating bath composition, bath additives, and deposition parameters). Additionally, a thorough knowledge of copper thin film morphology must be developed. Table 1 illustrates the National Technology Roadmap forecast for insertion of the various technology nodes (critical dimension of trenches).[1]

For copper electroplating to be extendible to the smaller feature sizes, 0.25 µm (9.75 µin) to 0.10 µm (3.9 µin), technology improvements become important, not only for electroplating, but for photolithography, etch, barrier and seed, and post plating chemical-mechanical polishing (CMP).

Currently, copper electroplating of interconnects is performed with a commercially available sulfuric acid-cupric sulfate solution utilizing proprietary additives similar to those used for the printed wire board process. Table 2 lists a typical composition for a copper plating solution used in the semiconductor manufacturing process.

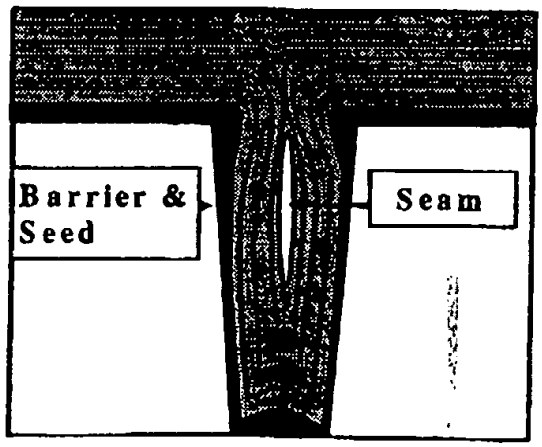

Fig. 1—Diagram of seam formation during conformal electroplating fill of re-entrant trench.

These solutions have demonstrated satisfactory electroplating fill for feature sizes down to ~0.20 µm (7.8 µin) with an aspect ratio (AR) of 4 (ratio of feature depth-to-width). Seam voids within the trenches and vias begin to appear during electroplating of features smaller than 0.20 µm (7.8 µin) and are partially related to the inability of the additive system to function properly in this regime. In contrast to plating of the through-holes in the printed wire boards, the plating of semiconductor devices requires filling of submicron blind vias and trenches. The small feature size and hydrodynamic conditions present for wafer plating dictate that a specifically optimized plating chemistry and bath additive package be developed for this application. Currently, a great deal of research and development is on-going at semiconductor facilities, universities, tooling suppliers, and chemical suppliers to develop new chemistries and to understand fully the electroplating deposition kinetics of the semiconductor interconnects. Ultimately, semiconductor grade copper plating solutions will be available with additives tailored to provide true leveling for void-free fill of interconnects.

Procedure

Currently, copper electroplating for semiconductor applications takes place typically on 200-mm (8 in.) silicon wafers with plans to shift processing eventually to 300-mm (12 in.) silicon wafers. Electroplating is performed in fully automated single-wafer platforms designed for high-volume manufacturing. Throughput for these tools is 10-12 wafers/hr/plating chamber, with most tools having 3-6 plating chambers. The plating process is designed to fill the features and provide sufficient overplate to achieve a high degree of leveling across the wafer. A post plating CMP process removes the copper overburden and prepares the wafer for the next layer processing. Multi-layer processing can have 6-9 layers of copper interconnects. Table 3 shows the processing steps required for single-layer processing.

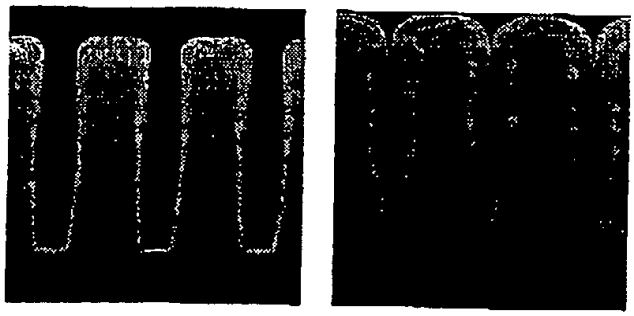

(SEM 1) (SEM 2)

Fig. 2—SEM cross section of 0.25 µm (9.75 µin) trench AR 4, showing seam formation during timed plating sequence; SEM 1 is after barrier & seed deposition, SEM 2 is after 10-sec plating.

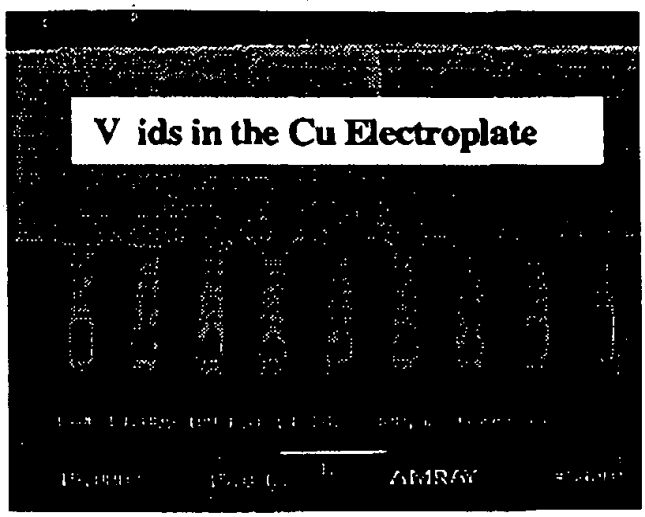

Fig. 3—Void formation as a result of thin PVD Cu seed layer on 0.25 µm (9.75 µin) AR 6 trench sidewall.

Results and Discussion

Electroplating Fill Defect Mechanisms

Electroplating defects are manifested as either vertical seams or voids in the trenches or vias. Seams are associated with a pinching off of the opening prior to fill of the structure. Voids are associated with poor step coverage of the copper seed layer.

Collimated physical vapor deposition (PVD) was used to deposit a 250 Å Ta barrier and a 1000 Å Cu seed on the wafers. Collimated PVD Cu deposition is an inherently non-uniform process that provides a step coverage of ~5-8 percent. Ideally, a minimum of ~100 Å of Cu seed on the trench lower sidewalls is sufficient for void-free electroplating fill. Deposition of 1000 Å of Cu seed provides ~50-80 Å of Cu seed on the lower sidewall of a 0.25 µm (9.75 µin) trench. Deposition of an excessive amount of copper seed at the feature opening can lead to a breadloafing effect, creating a re-entrant profile. Subsequent plating leads to seam voids. Figure 1 depicts the fill sequence for conformal fill of a re-entrant profile. Re-entrant etch profiles in the dielectric film will also lead to formation of seams during plating.

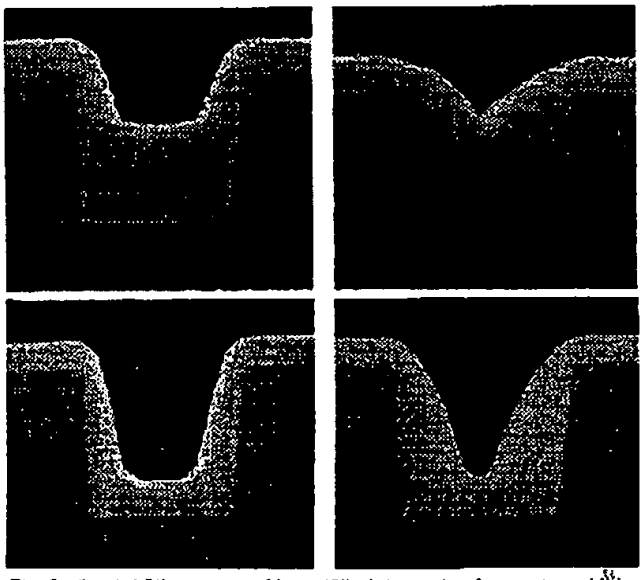

Fig. 5—Partial fill sequence of 1-µm (39 µin) trenches for varying additive levels deposited at 22 mA/cm² (20 ASF) for 20 sec. Top row: increased leveling agent; bottom row: increased suppressing agent.

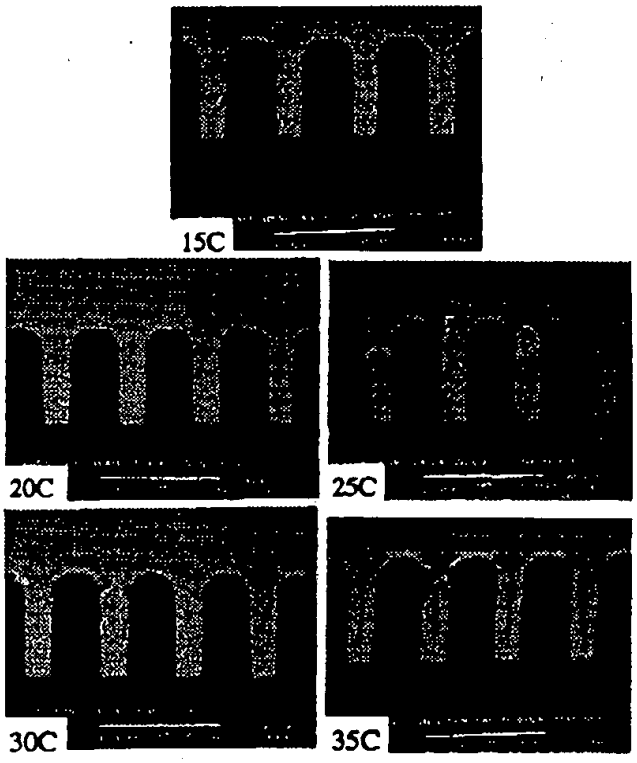

Fig. 4—Copper electroplating fill of 0.25-µm (9.75 µin) trenches, AR 4 at various temperatures.

The SEM cross sections in Fig. 2 show a partial fill of 0.25 µm (9.75 µin) re-entrant trenches. Examination of the PVD Ta barrier and Cu seed layer (SEM 1) reveals a re-entrant profile that leads to seam formation. SEM 2 shows that after 10 sec of plating, a seam is formed and that the fill mechanism is clearly conformal (*i.e.*, the deposition rate at the trench top is essentially equal to that at the sidewall). Under these conditions, there is little chance that the plating fill will be seam-free.

Voids are associated with insufficient bottom sidewall coverage by the PVD Cu seed. Thin (<50 Å) coverage on the bottom sidewall can result in dissolution of the Cu seed layer by the corrosive nature of the sulfuric acid-copper plating solution during initial immersion of a wafer. Voids are more

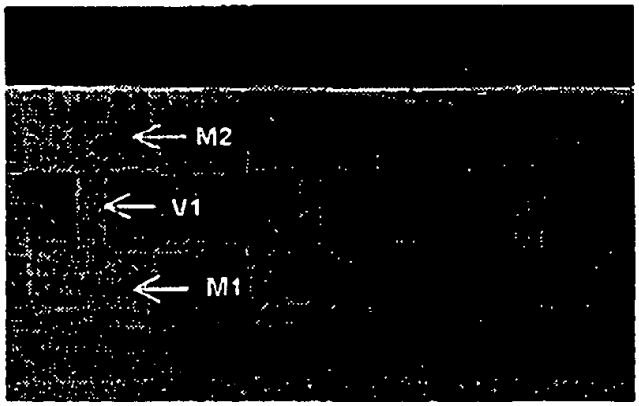

Fig. 6—Dual damascene fill: M1 (metal 1 layer), V1 (via 1), M2 (metal 2 layer.

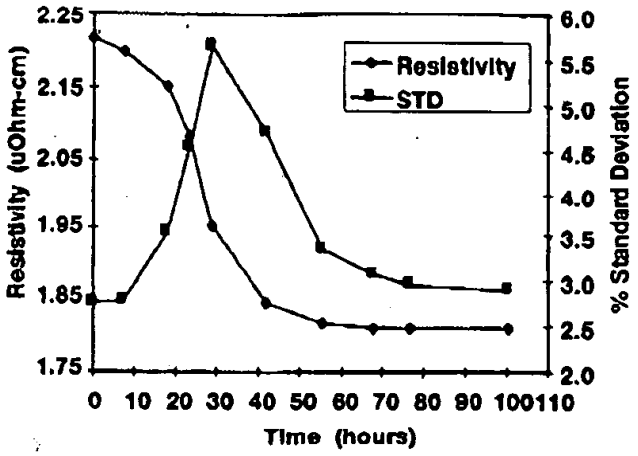

Fig. 7—Self-annealing effect on resistivity and standard deviation.

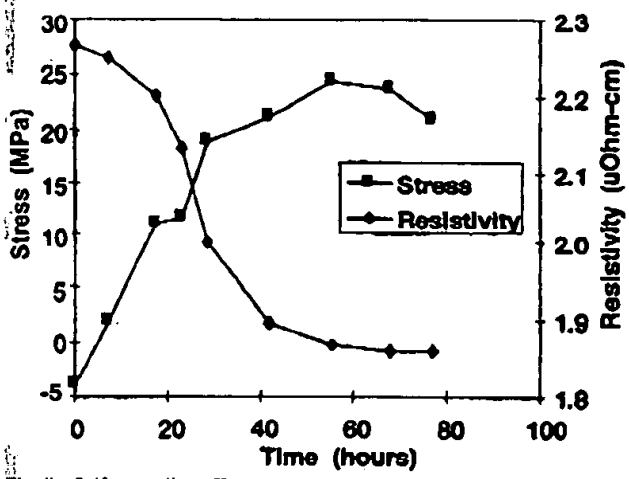

Fig. 8—Self-annealing effects on stress.

likely to occur during electroplating as the aspect ratio becomes large (AR > 6) and step coverage is minimal. Figure 3 shows the formation of voids near the trench bottom where the step coverage by the collimated PDV Cu seed was insufficient for electroplating. Use of hot entry or minimal solution exposure (solution dwell time) of the Cu seed prior to initiation of the deposition process can minimize the formation of voids.

Plated fill quality is affected by the operating temperature of the plating bath.[2] Figure 4 shows the copper fill of trenches over a temperature range of 15 to 35 °C. Optimum fill was obtained at 20 °C. Below 15 °C, reduction in mobility of the additive components may render them less effective and lead to seam formation. At temperatures of 30 °C and higher, the increased mobility of the suppressing agent may result in higher suppressor flux in the trench, which leads to enhanced conformal fill and seam formation.

Optimized Fill

Control of plating current density and additive levels in the bath has a dramatic effect on the fill mechanism. Figure 5 shows a series of partial fills of 1 µm (39 µin) trenches that have been plated at 22 mA/cm² (20 A/ft²) for 20 sec, with varying additive levels. Clearly, a higher concentration of leveling agent (top row SEM images) favored the formation of a bottom-up fill mechanism, while increased suppressing agents led to a diminished degree of bottom-up fill. In all cases, strong suppression or blocking of the deposition at the upper trench corners is apparent and is a necessary condition for void-free bottom-up fill. Figure 6 shows the cross section for a copper-plated dual damascene structure with a 0.25 µm (9.75 µin) via. The fill sequence for this structure consisted of a two-step fill process: Metal 1 (M1) was electroplated first, then Via 1/Metal 2 (V1/M2) were electroplated in one step after appropriate processing of M1 through CMP, lithography, and etch.

While copper deposited in the absence of additives will be columnar in structure and contain large grains, deposition in the presence of additives produces an equiaxed-fine-grained deposit. The additives used for copper electroplating are generally organic compounds that act as inhibitors, grain refiners, ductilizers and may be co-deposited with copper. Key components in most additive packages used for copper electroplating include the following:

Brighteners

Brighteners are generally organic compounds that contain sulfur and may also incorporate other functional groups. Examples include thiourea and derivatives of thiourea, 4,5-dithiooctane-1,8-disulfonic acid, mercapto-propane sulfonic

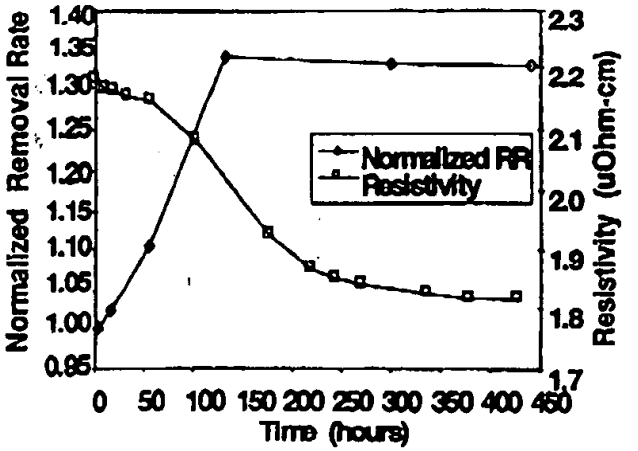

Fig. 9—CMP removal rate as a function of self-anneal time.

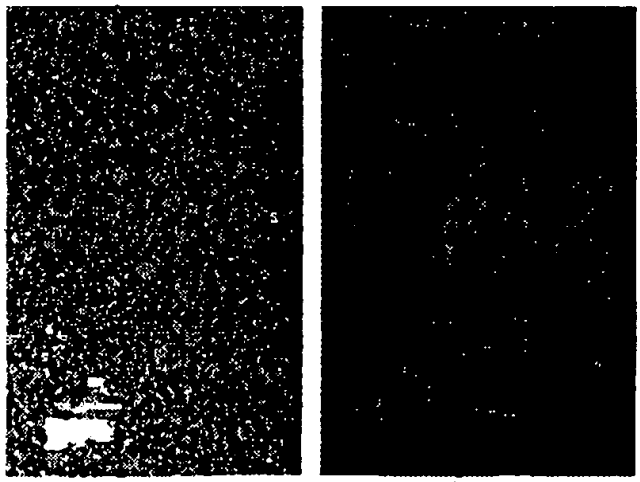

Fig. 10—Grain growth: (1) as-deposited grains ~0.1 µm (3.9 µin); (2) self-annealed grains > 1.0 µm (39 µin).

Fig. 11—Effect of 120 °C anneal on Cu grain size in 0.25 µm (9.75 µin) trenches.

acid.[3] Brighteners are responsible for the formation of small-grained, bright deposits. They function by preventing the deposition of copper at preferred locations by enhancing the formation of new deposit nuclei as opposed to the build-up of existing nuclei.

Levelers

Effective levelers tend to be medium molecular weight organic compounds containing key functional groups. They have low solubility in the plating solution, and have a low coefficient of diffusion. They act through selective adsorption on readily accessible surfaces (*i.e.*, flat field areas and protruding high points). The mechanism of leveling has been postulated elsewhere and numerous models have been developed to explain their mechanism, but it is generally accepted that true leveling is a result of diffusion control of the leveling species.[4-5] Examples of leveling agents include, but are not limited to, polyamines, such as derivatives of safronic dyes, with and without an OH functional group attached. Additives that function as brighteners and suppressors may also impart a slight measure of leveling to the deposit.[6]

Suppressing Agents

The characteristic of this additive component is formation of a continuous film on the surface that can completely block electrodeposition of copper. Suppressing agents are adsorbed on the wafer surface, forming a diffusion layer that limits the transfer of brighteners and levelers into the features, promoting their adsorption at the feature opening, resulting in true leveling. In the presence of chloride ions, the degree of adsorption and inhibition is further enhanced.[7] Suppressing agents include poly glycols such as polyethylene glycol, polypropylene glycol and co-polymers of polyglycols.[8-9] Suppressing agents are characterized by their high molecular weights, low solubility, and low coefficient of diffusion. The effectiveness of suppressing agents is a function of the molecular weight of the polymer; they must be tailored to the specific application.

Used alone, these additives have a minimal effect on the leveling of the deposit; however, formulated together they impart a synergistic effect that maximizes leveling effects.

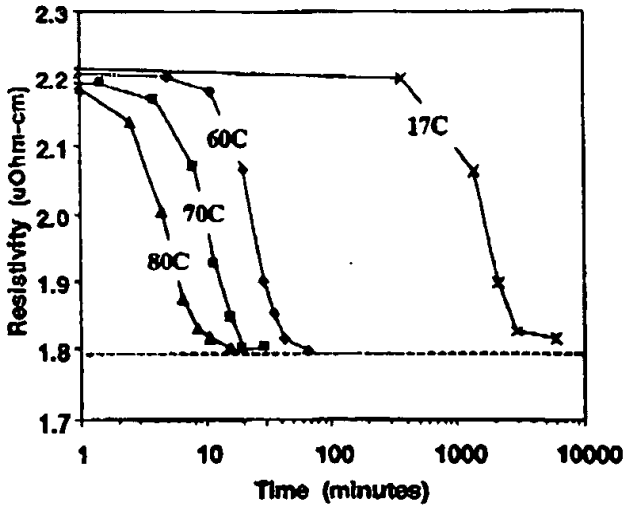

Fig. 12—Effects of thermal annealing on resistivity of the copper film.

Morphology of Electroplated Copper

It has been experimentally determined that a 1.5 µm (58.5 µin) electroplated copper film will self-anneal at room temperature in less than 50 hours.[10] Figure 7 shows the change in the resistivity of the copper film with time. The as-deposited bulk resistivity of electroplated Cu is ~2.22 microhm-cm and is stabilized at 1.80 microhm-cm approximately 50 hr later, a reduction of ~20 percent.

Associated with the change in resistivity is a transition in the non-uniformity (percent Standard Deviation) of the copper film from an initial value of ~3 percent (one sigma) to a maximum of ~5.5 percent (one sigma) during the midpoint of the self-annealing process and finally returning to ~3 percent (one sigma). Figure 8 shows that the stress changes from compressive to tensile. Figure 9 shows the CMP polishing rates for the copper films at various times after electrodeposition. There is an overall increase of 35 percent in the metal removal rate for the self-annealed copper attributed to a softening of the deposit with time (~40 percent reduction in hardness).

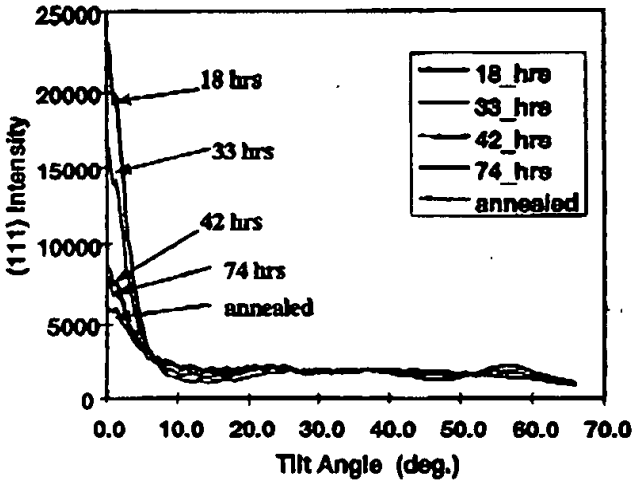

Fig. 13—Effects of self-anneal on fiber texture for 1.5 µm (58.5 µin) electroplated copper film.

The observed transformations in the electroplated 1.5 μm (58.5 μin) copper film are associated with the thermodynamic instability of the electroplated Cu film. The Cu film releases excess free energy through a complex process of recovery and recrystallization.[11] This transformation follows the Arrhenius equation,[12]

$$k = Ae^{-E_a/RT} \quad (1)$$

Where k is the rate constant, A is a constant, E is the activation energy, R is the universal gas constant and T is the temperature. Copper electroplated at mid-to-high current densities, 13-22 mA/cm² (11.8-20 A/ft²) in the presence of additives results in the formation of small-equiaxed grains containing a high density of defects. Increasing defect density increases the free energy, leading to a lowering of the activation energy required for recovery and recrystallization. As a result, the observed morphological transformations for the 1.5 μm (58.5 μin) copper film occurs at relatively low temperatures and times. The free energy is released through grain boundary annihilation. The final result is the transformation from small grains to large grains, reducing the number of grain boundaries, therefore improving the conductivity of the deposit. A softer deposit after self-annealing results in an overall improvement in the CMP metals removal rate. The grain growth is apparent in Fig. 10, which shows the as-deposited and self-annealed copper on a blanket wafer. The grain size ranges from ~0.1 μm (3.9 μin) for the as-deposited film to >1.0 μm (39 μin) for the self-annealed film. Figure 11 shows the grain growth within a trench after a 120 °C anneal. During the self-anneal process, the stress changes from compressive to tensile. The annihilation of the small grains and the formation of large grains results in a net decrease in deposit volume, which creates a tensile stress. Figure 12 shows the effects on the film stabilization by thermal annealing at various temperatures.

Figure 13 shows the effects of self-annealing and a post plating thermal anneal on the fiber texture of electroplated copper. Fiber texture plots for the electroplated copper film on blanket wafers showed an initial strong (111) orientation.[13] During the transition period for self-annealing, it is clear that the (111) texture decreases and the formation of secondary peaks is observed. Texture evolution is specific to the particular barrier material selected and may either strengthen with self-annealing or, as in this case, be reduced as a result of self-annealing. The morphological changes observed for thin electroplated copper films suggests the effect of a thermal annealing process for stabilization.

Summary

Copper electroplating is being implemented in the mainstream fabrication process for semiconductor devices. Copper electrodeposition has been successfully demonstrated as a viable alternative to the traditional aluminum metallization schemes. Semiconductor products will have been offered for commercial sale in 1999 that have electroplated copper for interconnects. Control of the electroplating fill mechanism is essential to the formation of defect-free copper deposits. Further development and optimization will be required to fully understand the interaction between the copper plating solution, organic additives, and the plating parameters to extend the electroplating capabilities from 0.25 μm (9.75 μin) down to 0.10 μm (3.9 μin) over the next several years. Additionally, control of the electroplated Cu microstructure is key to the manufacturing of reliable integrated circuits.

Editor's note: Manuscript received, March 1999.

References

1. *The National Technology Roadmap for Semiconductors*, Semiconductor Industry Assoc., p. 101 (1997).
2. Q.-T. Jiang, R. Mikkola & B. Carpenter, *1st International Conference on Advanced Materials and Processes for Microelectronics*, (March 1999).
3. E.E. Farndon, F.C. Walsh & S.A. Campbell, *J. Appl. Electrochem.*, 25 574 (1995).
4. Ken M. Takahashi, Mihal E. Gross, *Adv. Met. Conf.* (Oct. 1998).
5. C. Madore, M. Matlosz & D. Landolt, *J. Eletrochem. Soc.*, **143**(12), 3927 (1996).
6. L. Mirkova, St. Rashkov, CHR. Nanev, *Surf. Tech.*,**15**, 181 (1982).
7. G.Hope, G. Brown, *Proc. Electrochem. Soc.*, **96-8**, 215 (1996).
8. James Kelly & Alan West, *J. Electrochem. Soc.*, **145**(10), 3477 (1998).
9. J.D. Reid & A.P. David, *Plat. and Surf. Fin.*, **74**, 66, (1987).
10. Q.-T. Jiang, Robert Mikkola, Brad Carpenter & Michael Thomas, *Adv. Metal. Conf.* (1998).
11. B.M. Hogan, *Proc. AESF SUR/FIN '84, Session H* (1984).
12. Robert A. Alberty & Robert J. Silbey, *Physical Chemistry*, John Wiley and Sons Inc., New York, NY, 1997; p. 640.
13. Q.-T. Jiang, Robert Mikkola, Richard Ortega & Volker Blaschke, to be published.

About the Authors

Robert Mikkola is a staff engineer in the Metals Group at the Advanced Products and Research Laboratory, Motorola, 3501 Ed Bluestein Blvd., Austin, TX. For the past three years, he was on assignment at the international semiconductor research consortium, SEMATECH, in Austin, TX, where he was responsible for the implementation of copper electroplating technologies for advanced interconnects. He has been involved in metal finishing applications for the past 20 years, focusing on R&D, process development, and manufacturing support both in the semiconductor industry and the DOE weapons facilities in Oak Ridge, TN. He holds a BS chemistry and an MS in physical chemistry from Michigan Technological University.*

Dr. Q.T. Jiang is currently employed by Texas Instruments and is on assignment, working at the international semiconductor research consortium, Sematech, in Austin, TX. His work interests are in advanced back-end interconnects for microelectronics. He Holds a PhD in physics from Rutgers University.

Bradley Carpenter is a regional process engineer for Semitool, Inc. His responsibilities include performing tool start-ups, qualifications, process development, and optimization for semiconductor copper metalization. Additionally, he provides customer support for sustaining tools in manufacturing. He holds a BS in chemical engineering from the University of Minnesota and an MS in chemical engineering from the University of North Dakota.

* *To whom correspondence should be addressed.*

Journal of The Electrochemical Society, 150 (6) C435-C439 (2003)
0013-4651/2003/150(6)/C435/5/$7.00 © The Electrochemical Society, Inc.

Math matical Model of Galvanostatic Pulse with Rev rse Plating in the Presence of a Surface Blocking Agent

K.-M. Yin*,z

Department of Chemical Engineering, Yuan-Ze University, Neili, Taoyuan 32026, Taiwan

A theoretical model eliciting the effect of inert blocking inhibitors on the pulse with reverse plating of metal on the rotating disk electrode is presented. Additive inclusion rate during pulse period is determined by the metal deposition kinetics and the additive adsorption/inclusion characteristics. The release of incorporated additive during the reverse period can be determined by a mass conservation on addition agent in the deposited metal matrix, as derived in the paper. The potential response and average inclusion rate of the blocking agent can be predicted using this model.

Manuscript submitted August 28, 2002; revised manuscript received January 15, 2003. Available electronically April 22, 2003.

Current pulse with intermittent current-off (PC) is widely used in the plating industry of electronics.[1-6] It has been found that the mass-transport limitation or concentration depletion in the diffusion layer near the electrode surface can be alleviated at the presence of a current-off period. In recent development of multiplayer printed circuit boards in communication devices or computers, there is a need for high-density interconnections to minimize the size of products. One of the key plating techniques is to use pulse with reverse current (PR) for the interconnections of through-holes or blind vias across the circuit board.[7-9] That is, instead of a current-off, a reverse anodic current is applied in the relaxation period. The adoption of a reverse current selectively dissolves the protrusions of the metal surface to ensure a uniform deposit. This is especially important to the films on walls of through-holes with high aspect ratios. In addition, various addition agents of strong adsorption characteristics are always added in the bath to increase the throwing power on the far recessed area. The use of reverse pulse in the presence of organic surface agent is the recent electronics surface finishing practice.[10,11] However, there is also a need to reduce the use of organic additives in printed circuits and in the damascene metallization of submicrometer interconnects in semiconductors,[12,13] because the organic material incorporated in the solid phase could damage the electronic properties of the deposit film such as conductivity, ductility, and adhesion. In view of the importance of pulse with reverse technique and the imperative but reluctant use of organic agent, it is most helpful to have a mathematical model of pulse with reverse plating that is capable of predicting the incorporation rate of organic agent in the deposit.

The most important feature of organic surfactant is its strong adsorption property on the electrode surface to increase surface activation overpotential. The blocking agent was studied theoretically and experimentally at steady state dc condition as early as the 1950s.[14-26] The most agreed upon mechanism of addition agent is its "dirt-blocking" effect[21] based on the increased surface activation overpotential. The blocking effect may be diminished at higher applied potential when additive incorporation rate reaches its mass-transfer-limited condition, while metal reduction rate is still increased steadily. Kruglikov *et al.*[19] proposed that the rate of inclusion is given by

$$N_{inc} = \frac{k_i}{F}\theta_{add}i \qquad [1]$$

where i is the applied apparent current density, θ_{add} the fractional surface coverage of additive, and k_i the inclusion rate constant. This equation was modified later by replacing the apparent current density with intrinsic current density $i/(1-\theta_{add})$,[22-24] as given by Eq. 6 in the present paper. This treatment implies that the additive is electrochemically inert to the electrode and does not change its oxidation state. However, some researchers do not consider the addition agent to be inert, that is, that the additive has its own electrochemical characteristics in the incorporation step. It is then possible for the included material to be different from the original state of additive in the bath.[15,18]

Although rigorous treatment of the additive effect in dc plating exists, accounts of the effect of addition agent in the mode of pulse plating are rare. It was pointed out by Delahay and Fike[27] that in general, adsorption equilibrium is reached slowly except when the additive concentration is at least ten times larger than the inverse of adsorption equilibrium constant K_a of the Langmuir isotherm. It is expected that the adsorption behavior of additive agent in pulse plating is much more important than that of dc. Yin[28] proposed a mathematical model that considered the effect of organic additive in the pulse without reverse plating (PC). The purpose of the present study is to extend the previous work to simulate the additive adsorption and incorporation phenomena as a function of metal deposition and additive adsorption kinetics on the PR from the first principle.

Mathematical Model

In the present study, the addition agent is assumed inert, which is incorporated in the deposit through the reduction of metal ion species. That is, the oxidation state of additive in the deposit is not different from that in the bulk solution. The "inert" assumption, however, can be removed from the model if the individual kinetic expression is available for the addition agents that do participate in certain electrochemical reactions. Other assumptions are listed as follows: (*i*) The double-layer charging/discharging effect is not considered. This capacitance effect can be added with ease, for example, see Ref. 29 and 30. (*ii*) Dilute solution theory applies in the electrolytes; that is, no interaction exists between ionic species. (*iii*) Migration effect in the solution phase is unimportant. (*iv*) The solution is isothermal, and the mass-transfer and kinetics parameters are constant throughout the system.

A one-dimensional model on a rotating disk electrode (RDE) is considered. The sign convention of flux quantity in this paper follows the positive y coordinate, that is, a positive value is assigned if flux is in the normal direction from the electrode surface to electrolyte. The mass conservation for metal ion or addition agent within the diffusion layer is expressed as

$$\frac{\partial C_i}{\partial t} = D_i\frac{\partial^2 C_i}{\partial y^2} - v_y\frac{\partial C_i}{\partial y} \qquad [2]$$

The convection induced by the RDE is approximated by the first term of a power series $v_y = -0.51023\,\Omega^{1.5}\nu^{-0.5}y^2$. Ω is the disk rotation rate in rad/s, ν is solution kinematic viscosity, and y is the distance from electrode surface.[31]

The electrode surface kinetics for metal reduction or dissolution is related to the surface fraction of unblocked area $(1-\theta_{add})$, interfacial reactant concentration $C_{M^{n+}s}$, and electrode potential E[28]

* Electrochemical Society Active Member.
z E-mail: cekenyin@tutum.yzu.edu.tw

$$-N_{M^+} = D_{M^+}\left.\frac{\partial C_{M^+}}{\partial y}\right|_{y=0} = \frac{i_o}{F}(1-\theta_{add})\left\{\frac{C_{M^+s}}{C_{M^+b}}\exp\left(-\frac{\alpha_c F}{RT}E\right) - \exp\left(\frac{\alpha_a F}{RT}E\right)\right\} \quad [3]$$

where i_o is the exchange current density for a reversible reaction corresponding to the bulk concentrations, C_{M^+s}/C_{M^+b} is the dimensionless concentration of M^+ at the interface, and α_c and α_a are the apparent cathodic and anodic charge-transfer coefficients, respectively.

The adsorption rate of the additive is expressed as follows

$$-N_{add} = D_{add}\left.\frac{\partial C_{add}}{\partial y}\right|_{y=0} = k_a C_{add,s}\Gamma(1-\theta_{add}) - k_d\Gamma\theta_{add} \quad [4]$$

where k_a and k_d are the respective adsorption and desorption rate constants of additive, which are potential-independent. Γ is the adsorbed additive concentration of one complete monolayer, and $C_{add,s}$ is the solution additive concentration at the interface.

The surface concentration of adsorbed blocking agent is a function of time. During the pulse period (t_p), the number of surface-accumulated additives is the difference between the rate of additive adsorption onto the surface and the inclusion rate of adsorbed surface additives

$$\Gamma\frac{d\theta_{add}}{dt} - N_{ip} - (-N_{add}) = 0 \quad [5]$$

where the inclusion rate of additive $-N_{ip}$ during the pulse period is given by[22-24]

$$N_{ip} = \frac{k_i}{F}\theta_{add}\frac{i_p}{1-\theta_{add}} \quad [6]$$

where k_i is the inclusion rate constant, and i_p is pulse current density with a negative value in the electrochemical convention. The inclusion rate in the pulse period is a function of surface coverage of blocking agent, θ_{add}, and the intrinsic current density $i_p/(1-\theta_{add})$. k_i is related to the surface concentration of one complete monolayer of adsorbed additive[22,23]

$$k_i = \frac{\Gamma M_w}{d_a\rho} \quad [7]$$

where M_w and ρ are the metal atomic weight and density, respectively, and d_a is the diameter of addition agent.

In the reverse period (t_r), instead of inclusion, additive is released from the metal matrix to the interface as the adsorbed state. Mass balance on the surface-adsorbed additive in the reverse period can be expressed similar to Eq. 5, that is

$$\Gamma\frac{d\theta_{add}}{dt} - N_{ir} - (-N_{add}) = 0 \quad [8]$$

N_{ir} is the release rate of embedded additive in the reverse period. To obtain the expression of $N_{ir}(t)$ in the reverse period, one may apply a mass conservation law to the solid metal phase and to the included additives. As shown in Fig. 1, set the beginning of a reverse period as t_{ref}, then the total charge passed from t_{ref} until t is equal to $i_r(t-t_{ref})$, and the solid surface at time t corresponds to a time t' in the previous pulse period. t' can be determined as follows

$$i_r(t-t_{ref}) = |i_p|(t_{ref}-t') \quad [9]$$

A similar mass conservation is applied to the additives within the metal matrix

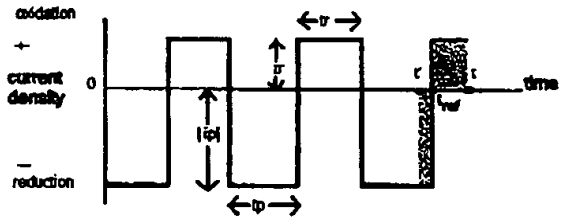

Figure 1. Schematic diagram of a typical pulse with reverse waveform.

$$\int_{t_{ref}}^{t} N_{ir}(\tau)d\tau = \int_{t'}^{t_{ref}}|N_{ip}(\tau)|d\tau \quad [10]$$

Taking derivatives on both sides of Eq. 10 with respect to t in Leibnitz's formula,[32] one obtains

$$N_{ir}(t) = N_{ip}(t')\frac{dt'}{dt} \quad [11]$$

With the aid of Eq. 9, Eq. 11 becomes

$$N_{ir}(t) = N_{ip}(t')\frac{i_r}{i_p} \quad [12]$$

Equation 12 indicates that the release rate of additives from the solid phase at time t in the reverse period can be calculated from the incorporation rate of additives in the previous pulse period at time t'. Numerically, $N_{ir}(t)$ can be calculated once $N_{ip}(t')$ is determined by interpolation in the previous pulse period. Cubic spline interpolation with natural boundary is used in the present model.[33]

Finally, the periodic current density applied accounts for the reduction of metal ion, or oxidation of solid metal

$$N_{M^+} = \frac{i(t)}{F} \quad [13]$$

where $i(t) = i_p$ in pulse period, and $i(t) = i_r$ in reverse period.

The governing equations and the associated boundary conditions described are discretized in the finite difference form and then solved by a matrix solver named BAND coupled with a Newton-Raphson iteration scheme.[31] Fixed parameters used in the simulation are listed in Table I.

Results and Discussion

To simplify the discussion of the problem, only irreversible addition agent adsorption is considered, that is, $k_d = 0\ s^{-1}$. The initial condition is set that before current is applied, the disk is rotated at a constant speed and the fractional coverage of additive is unity. The

Table I. Fixed parameters used in the simulation.

$y_{\infty} = 0.01$ cm	$\alpha_c = 0.5$
$\nu = 0.01$ cm^2 s^{-1}	$\alpha_a = 0.5$
$T = 298$ K	$D_{M^+} = 1\times10^{-5}$ cm^2 s^{-1}[d]
$i_o = 1\times10^{-8}$ A cm^{-2}[a]	$D_{add} = 1\times10^{-6}$ cm^2 s^{-1}[d]
$d_a = 3\times10^{-7}$ cm[b]	$C_{M^+bulk} = 1.5\times10^{-4}$ mol cm^{-3}[e]
$\rho = 7.9$ g/cm^3[c]	$C_{add,bulk} = 1\times10^{-6}$ mol cm^{-3}[e]
$M_w = 55.85$ g/mol[c]	

[a] Chosen arbitrarily.
[b] Chosen as ten times of iron atomic diameter.
[c] Property of iron, the value of which is common in most transition metals.
[d] Commonly used diffusion coefficients in solution.
[e] Commonly used bath concentrations.

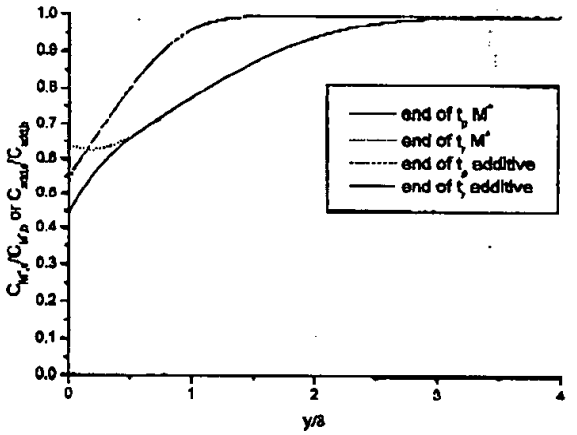

Figure 2. Dimensionless concentration profiles of the metal-additive deposition system on the RDE: $k_i = 1 \times 10^{-3}$, $k_a = 5 \times 10^7$ cm^3 mol^{-1} s^{-1}, $t_p = 10$ ms, $t_r = 10$ ms, $i_p = -80$ mA cm^{-2}, $i_r = 20$ mA cm^{-2}, 298 K, 500 rpm. δ is defined as $(3D_{add}/av)^{1/3}(\nu/\Omega)^{1/2}$.

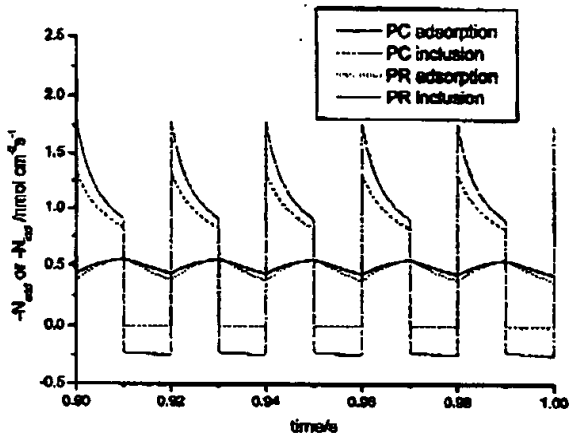

Figure 4. Additive adsorption and incorporation rates as a function of time. Key as in Fig. 3.

calculation is terminated once the periodic steady state is attained. The establishment of the periodic steady state is ensured as the relative changes of surface concentrations of metal ion and additive, surface coverage, and electrode potential are all less than 0.1% between two sequential cycles. The checkpoint chosen is the end of each reverse period.

Figure 2 depicts the dimensionless concentration profiles of metal ion, M^+, and additive within the diffusion layer at the end of t_p and at the end of t_r when periodic steady state is achieved. It is shown that metal dissolves at the reverse period, causing metal ion accumulation near the electrode. Compared to dc or PC mode, the buildup of metal ion during t_r reduces the concentration overpotential for the subsequent pulse period. At the given operating condition, the additive consumption rate by incorporation into the solid phase is relatively low, and there is less concentration depletion about the additives. It is shown that the variation of blocking agent concentration is minor within a cycle.

Figure 3 is a comparison of potential responses of PR and PC in the presence or absence of organic additive. For PC mode, the potential during t_p is more cathodic for the blocking agent added bath than that without additive, which accounts for the increased surface activation overpotential caused by the surface-adsorbed additive. The same is observed for PR mode. That is, in the PR pulse period, the one with additive has larger cathodic polarization than that without additive. There is also an increased anodic polarization in the additive-included bath during the reverse period for PR mode. Note that additive has no effect on the potential response during t_{off} in the PC mode because no current is applied in that period. Thus, the electrode voltages during t_{off} coincide with each other in the additive-included and -absent baths in PC mode. It is interesting to know that in PR mode, the potential difference between the baths with and without additive decreases along the progress of pulse time, while the opposite is true in the reverse time. The reason is that during t_p the surface-adsorbed agent is continuously incorporated into the metal matrix, causing the reduction of surface blockage of additive with time. As a result, the surface activation potential is decreased with pulse time. During the reverse period, some of the included organic agents are released from the solid phase and become part of the surface-blocking layer. Thus, in the reverse time, the surface additive coverage is increased by the contributions of adsorbed agents from solution plus that released from the metal matrix. One may also compare PC with PR at the additive-absent baths. The deviation of potential in pulse period between the two comes from the larger concentration overpotential in PC mode due to the less supply of metal ion during off-time than that of reverse time in PR mode, as illustrated in Fig. 2.

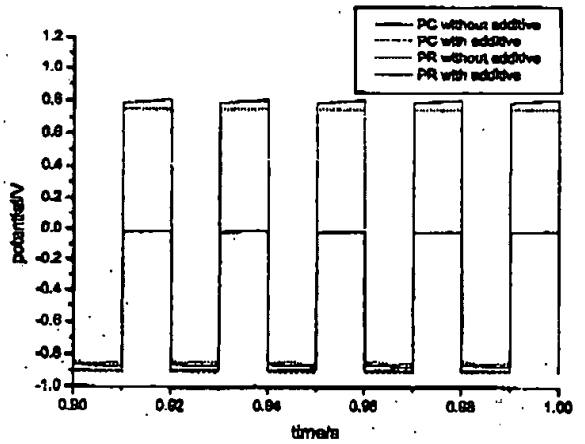

Figure 3. Potential responses as a function of time. Operating parameters are the same as Fig. 2 except that for PC mode, the current density is set to zero at the off-time.

Figure 4 shows the typical periodic adsorption and inclusion rates of additive. It is shown that in pulse period, PR mode has a higher inclusion rate than that of PC mode. The inclusion rate decreases along the pulse time because surface coverage of the additive decreases with pulse time. No additive is included during off-time in PC mode since no current passed in that period. While in the reverse period of PR mode, additives released from the solid matrix increase steadily with time. The release rate depends on the history of previous pulse inclusion rates according to Eq. 12. The adsorption rate for PC is always higher than in PR mode in a complete cycle. This implies that the average inclusion rate over one cycle is less in PR mode than in PC mode. Note that in either PR or PC mode, the overall inclusion rate of additive in one cycle is equal to that of the adsorption rate as periodic steady state is achieved, that is

$$\int_{\text{one cycle}} -N_{add}dt = \int_{\text{one cycle}} -N_{inc}dt \qquad [14]$$

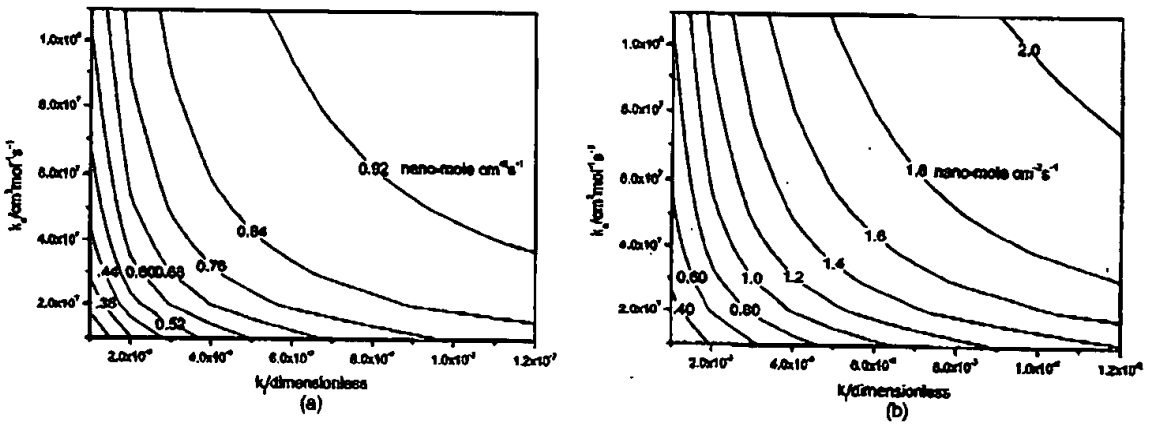

Figure 5. Average inclusion rate as a function of adsorption and incorporation rate constants: (a, left) 500 and (b, right), 2500 rpm. t_p = 10 ms, t_r = 10 ms, i_p = −80 mA cm^{-2}, i_r = 20 mA cm^{-2}, 298 K.

Figure 5a and b depicts the effects of adsorption rate constant and inclusion rate constant on the average additive inclusion rate at disk rotation speeds of 500 and 2500 rpm. It is shown that the average inclusion rate increases at the increase of k_a and k_i. As indicated in Fig. 5a, for a specified k_a, *e.g.*, 1×10^{-8} cm^3 mol^{-1} s^{-1}, a steady increase of k_i indeed enhances the inclusion rate of addition agent. However, the rate of change of inclusion rate decreases with k_i, suggesting that mass-transfer effect plays a more significant role as k_i increases. A similar argument is applied to the effect of k_a on the additive inclusion rate for a specified k_i value. For a comparison of Fig. 5b with a, one can see that the inclusion rate is generally much increased if a larger disk spinning rate is employed. No significant mass-transfer limitation is observed until an inclusion rate of 1.8 nano-mol cm^{-2} s^{-1} is reached for a disk speed of 2500 rpm.

Conclusion

A theoretical study of galvanostatic pulse with reverse plating on RDEs in the presence of an inert blocking agent is presented in this paper. This model is capable of predicting the release of additive in the reverse period. It is shown that the model can be used to evaluate the average inclusion rate of organic material as a function of general pulse operating conditions.

Acknowledgments

The author is grateful for financial support by the National Science Council of the Republic of China (NSC-90-2214-E-155-008). Helpful discussions with Lili Cheng are also appreciated.

Yuan-Ze University assisted in meeting the publication costs of this article.

List of Symbols

a 0.51023
C_i concentration of species i, mol cm^{-3}
d_a additive diameter, cm
D_i diffusion coefficient of species i, cm^2 s^{-1}
E electrode potential, V
F Faraday constant, 96,500 C mol^{-1}
i applied current density, A cm^{-2}
i_o exchange current density of metal deposition, A cm^{-2}
i_p current density in pulse period, A cm^{-2}
i_r current density in reverse period, A cm^{-2}
k_a additive adsorption rate constant, cm^3 mol^{-1} s^{-1}
k_d additive desorption rate constant, s^{-1}
k_i additive inclusion rate constant, dimensionless
K_a adsorption equilibrium constant, k_a/k_d, cm^3 mol^{-1}
M_w atomic weight of metal, g mol^{-1}
N_{add} additive adsorption rate, mol cm^{-2} s^{-1}
N_{incl} additive inclusion rate, mol cm^{-2} s^{-1}
N_{ip} additive inclusion rate in pulse period, mol cm^{-2} s^{-1}
N_{ir} additive release rate in reverse period, mol cm^{-2} s^{-1}
N_{M^+} metal ion flux, mol cm^{-2} s^{-1}
R gas constant, J mol^{-1} k^{-1}
t time, s
t_{off} off-time in pulse without reverse mode, s
t_p pulse time, s
t_r reverse time, s
T absolute temperature, k
v_y normal fluid velocity, cm s^{-1}
y_{ro} reference position where no concentration gradient of species exists, cm

Greek

α_a anodic transfer coefficient, dimensionless
α_c cathodic transfer coefficient, dimensionless
Γ surface-adsorbed additive concentration of one monolayer, mol cm^{-2}
ν kinematic viscosity of solution, cm^2 s^{-1}
θ_{add} additive surface fractional coverage, dimensionless
ρ metal density, g cm^{-3}
Ω disk rotation speed, rad s^{-1}

References

1. H. Y. Cheh, *J. Electrochem. Soc.*, **118**, 551 (1971).
2. N. Ibl, *Surf. Technol.*, **10**, 81 (1980).
3. D. Landolt, in *Theory and Practice of Pulse Plating*, J. C. Puippe and F. Leaman, Editors, p. 55, American Electroplaters and Surface Finishers Society, Orlando, FL (1986).
4. K.-M. Yin and R. E. White, *AIChE J.*, **36**, 187 (1990).
5. C.-C. Yang and H. Y. Cheh, *J. Electrochem. Soc.*, **142**, 3034 (1995).
6. C.-C. Yang and H. Y. Cheh, *J. Electrochem. Soc.*, **143**, 3040 (1995).
7. J. Barthelmes, *Trans. Inst. Met. Finish.*, **78**(4), 135 (2000).
8. B. J. Taylor, J. J. Sun, and M. E. Inmar, *Plat. Surf. Finish.*, **2000**, 68 (Dec).
9. S.-C. Kou and A. Hung, *Plat. Surf. Finish.*, **2000**, 140 (May).
10. E. Gutierrez, *CircuiTree*, **2001**, 46 (April).
11. G. Milad, *PC FAB*, **20**, 36 (1997).
12. A. C. West, C.-C. Cheng, and B. C. Baker, *J. Electrochem. Soc.*, **145**, 3070 (1998).
13. B. J. Taylor, J. Sun, B. Hammack, and C. Davidson, *CircuiTree*, **2001**, 36 (May).
14. D. G. Foulke and O. Kardos, *Proc. Am. Electrepl. Soc.*, **43**, 172 (1956).
15. S. E. Beacom and B. J. Riley, *J. Electrochem. Soc.*, **108**, 758 (1961).
16. O. Kardos and D. G. Foulke, in *Advances in Electrochemistry and Electrochemical Engineering*, P. Delahay and C. W. Tobias, Editors, Vol. II, Interscience, New York (1962).
17. S. S. Kruglikov, N. T. Kudriavtsev, O. F. Vorobiova, and A. Ya. Antonov, *Electrochim. Acta*, **10**, 253 (1965).
18. G. T. Rogers and K. J. Taylor, *Electrochim. Acta*, **11**, 1685 (1966).
19. S. S. Kruglikov, Yu. D. Gamburg, and N. T. Kudryavtsev, *Electrochim. Acta*, **12**, 1129 (1967).
20. S. S. Kruglikov, N. T. Kudryavtsev, and R. P. Sobolev, *Electrochim. Acta*, **12**, 1263 (1967).
21. T. C. Franklin, J. Chappel, R. Fierro, A. I. Aktan, and R. Wickham, *Surf. Coat. Technol.*, **34**, 515 (1988).
22. D. Roha and U. Landau, *J. Electrochem. Soc.*, **137**, 824 (1990).

23. J. O. Dukovic and C. W. Tobias, *J. Electrochem. Soc.*, 137, 3748 (1990).
24. K. G. Jordan and C. W. Tobias, *J. Electrochem. Soc.*, 138, 1251 (1991).
25. C. Madore, M. Matlosz, and D. Landolt, *J. Electrochem. Soc.*, 143, 3927 (1996).
26. C. Madore, M. Matlosz, and D. Landolt, *J. Electrochem. Soc.*, 143, 3936 (1996).
27. P. Delahay and C. T. Fike, *J. Am. Chem. Soc.*, 80, 2628 (1958).
28. K. M. Yin, *J. Electrochem. Soc.*, 145, 3851 (1998).
29. W.-C. Tsai, C.-C. Wan, and Y.-Y. Wang, *J. Electrochem. Soc.*, 149, C229 (2002).
30. N. Tantavichet and M. D. Pritzker, *J. Electrochem. Soc.*, 149, C289 (2002).
31. J. S. Newman, *Electrochemical Systems*, 2nd ed., p. 315 and 545, Prentice-Hall, Englewood Cliffs, NJ (1991).
32. F. B. Hildebrand, *Advanced Calculus for Applications*, 2nd ed., p. 365, Prentice-Hall, Englewood Cliffs, NJ (1976).
33. G. E. Forsythe, M. A. Malcolm, and C. B. Moler, *Computer Methods for Mathematical Computations*, p. 76, Prentice Hall, Englewood Cliffs, NJ (1977).